Original Article

Changes in Liver Ganglioside Metabolism in Obstructive Cholestasis – the Role of Oxidative Stress

(cholestasis / gangliosides / haem oxygenase / liver)

V. ŠMÍD[1,2], T. PETR[1], K. VÁŇOVÁ[1], J. JAŠPROVÁ[1], J. ŠUK[1], L. VÍTEK[1,2], F. ŠMÍD[1], L. MUCHOVÁ[1]

[1]Institute of Medical Biochemistry and Laboratory Diagnostics, [2]4th Department of Medicine, First Faculty of Medicine, Charles University in Prague and General University Hospital in Prague, Czech Republic

Abstract. Bile acids have been implicated in cholestatic liver damage, primarily due to their detergent effect on membranes and induction of oxidative stress. Gangliosides can counteract these harmful effects by increasing the rigidity of the cytoplasmic membrane. Induction of haem oxygenase (HMOX) has been shown to protect the liver from increased oxidative stress. The aim of this study was to determine the changes in the synthesis and distribution of liver gangliosides following bile duct ligation (BDL), and to assess the effects of HMOX both on cholestatic liver injury and ganglioside metabolism. Compared to controls, BDL resulted in a significant increase in total as well as complex gangliosides and mRNA expression of corresponding glycosyltransferases ST3GalV, ST8SiaI and B3GalTIV. A marked shift of GM1 ganglioside from the intracellular compartment to the cytoplasmic membrane was observed following BDL. Induction of oxidative stress by HMOX inhibition resulted in a further increase of these changes, while HMOX induction prevented this effect. Compared to BDL alone, HMOX inhibition in combination with BDL significantly increased the amount of bile infarcts, while HMOX activation decreased ductular proliferation. We have demonstrated that cholestasis is accompanied by significant changes in the distribution and synthesis of liver gangliosides. HMOX induction results in attenuation of the cholestatic pattern of liver gangliosides, while HMOX inhibition leads to the opposite effect.

Corresponding author: Lucie Muchová, Institute of Medical Biochemistry and Laboratory Diagnostics, First Faculty of Medicine, Charles University in Prague and General University Hospital in Prague, Kateřinská 32, 121 08 Prague 2, Czech Republic. Phone: (+420) 224 964 199; Fax: (+420) 224 962 532; e-mail: lucie.muchova@lf1.cuni.cz

Abbreviations: aBDL – BDL with HMOX activation, aC – control with HMOX activation, ALP – alkaline phosphatase, ALT – alanine aminotransferase, AST – aspartate aminotransferase, B3GalTIV – UDP-Gal:βGlcNAc β 1,3-galactosyltransferase, B4GalNTI – β-1,4-N-acetyl-galactosaminyl transferase 1, BA – bile acids, BDL – bile duct ligation, BSA – bovine serum albumin, C – control, cAMP, cyclic adenosine monophosphate, CO – carbon monoxide, CTB – cholera toxin B-subunit, EDTA – ethylenediamine tetraacetic acid, EE – 17α-ethinyl oestradiol, FW – fresh weight, GalTI – UDP-Gal:βGlcNAc β 1,4-galactosyltransferase, GlcT – UDP-glucose ceramide glucosyltransferase, GSL – glycosphingolipids, HMOX – haem oxygenase, iBDL – BDL with HMOX inhibition, iC – control with HMOX inhibition, PBS – phosphate-buffered saline, ROS – reactive oxygen species, SnMP – tin-mesoporphyrin, ST3GalV – ST3 β-galactoside α-2,3-sialyltransferase 5, ST8SiaI – ST8 α-N-acetyl-neuraminide α-2,8-sialyltransferase 1, TBA – total bile acids. GSL are abbreviated according to the recommendations of the IUPAC-IUB Commission on Biochemical Nomenclature (Chester, 1998)

Introduction

Cholestasis is an impairment of bile secretion and/or flow, followed by a lack of bile in the intestine and accumulation of potentially toxic bile acids (BA) in the liver and systemic circulation (Paumgartner, 2006). A major consequence of cholestasis is development of severe liver injury due to rapid accumulation of BA within the hepatocytes (Gujral et al., 2003). It is generally assumed that the exposure of hepatocytes to high concentrations of potentially toxic BA is primarily responsible for cholestatic liver injury (Perez and Briz, 2009). The molecular mechanisms behind early liver injury associated with cholestasis have been extensively studied, but are still not well understood (Woolbright and Jaeschke, 2012). BA act as an inflammation agent, directly activating the signalling pathways in hepatocytes that regulate production of proinflammatory mediators (Allen et al., 2011). Recent data support the hypothesis that cholestatic liver injury may not occur through direct BA-induced apoptosis, but may mainly involve inflammatory cell-

mediated liver cell necrosis (Woolbright and Jaeschke, 2012).

Equally, amphipathic BA could disrupt cell membranes and cause structural and/or functional damage of the hepatocyte membrane through their detergent action on lipid components (Billington et al., 1980). Another mechanism for the development of cholestatic liver injury arises from ultrastructural changes such as altered cell polarity, disruption of cell-to-cell junctions, cytoskeletal changes, and membrane fluidity (Trauner et al., 1999).

More than 30 years ago, decreased fluidity of the cytoplasmic membrane in erythrocytes of patients with intrahepatic cholestasis (Balistreri et al., 1981), as well as in the livers of mice with intrahepatic cholestasis (Boelsterli et al., 1983), was described. Changes in the membrane cholesterol and sphingomyelin contents were at least partially responsible for these changes (Smith and Gordon, 1988).

It is known that cholesterol-(glyco)sphingolipid (GSL) complexes, tightly packed in a liquid ordered state (Munro, 2003; Rajendran and Simons, 2005), called lipid rafts, are needed to protect the membranes against the detergent effect/action of BA (Guyot and Stieger, 2011).

Gangliosides, forming a major part of GSL, are assembled from a lipophilic ceramide portion plus a structurally variable hydrophilic oligosaccharide portion containing N-acetylneuraminic acid. They are highly concentrated in the outer layer of the plasmatic membrane, and thanks to their unique physical and chemical properties, they are considered crucial molecules responsible for the rigidity of plasmatic membranes (Pascher, 1976; Pascher et al., 1992).

The possible relationship between decreased membrane fluidity and changes in the content and localization of GSL in intrahepatic cholestasis was recently investigated by our group (Jirkovska et al., 2007). Based on this study, the redistribution of gangliosides on the sinusoidal membrane of the hepatocyte seems to be a protective mechanism of hepatocytes against the harmful effects of BA accumulated during ethinyl oestradiol (EE)-induced cholestasis. A significant increase of total lipid sialic acid – the hallmark of ganglioside content – together with a high increase of gangliosides synthesized in the so-called b-biosynthetic pathway (Fig. 1) was found in EE-induced cholestasis in rats (Majer et al., 2007). These results suggest that changes in the localization and content of gangliosides may serve as a protective mechanism against cholestatic liver injury.

Moreover, our recent data also indicate that the changes and redistribution of gangliosides during experimental EE-induced cholestasis are attributable to high concentrations of accumulated BA (Jirkovska et al., 2007), as well as increased oxidative stress (Petr et al., 2014) in the EE-induced cholestasis model. One of the important anti-oxidant and anti-inflammatory factors is haem oxygenase (HMOX; E.C. 1:14:99:3). HMOX catalyses the rate-limiting step in the oxidative degradation of haem, converting it into biliverdin IXα and subsequently to bilirubin IXα by biliverdin reductase (E.C. 1:3:1:24), carbon monoxide, and iron. HMOX plays a key role in the cellular and tissue defences against oxidative stress (Poss and Tonegawa, 1997). Upregulation of its inducible isoenzyme HMOX-1 has been shown to protect the liver from toxic, inflammatory, and oxidative insults. Recently, we have shown that BA are potent inhibitors of HMOX activity and expression (Muchova et al., 2011). The decreased HMOX activity in the cholestatic liver causes relative depletion of intracellular bilirubin, a potent endogenous antioxidant (Vitek et al., 2002). The relative lack of this intracellular antioxidant together with high levels of pro-oxidative BA participates in the pathogenesis of oxidative stress-mediated liver injury. In addition, we reported the anticholestatic effect of HMOX induction (Muchova et al., 2015) as well as restoration of the changes in the synthesis and distribution of gangliosides in EE-induced cholestasis (Petr et al., 2014).
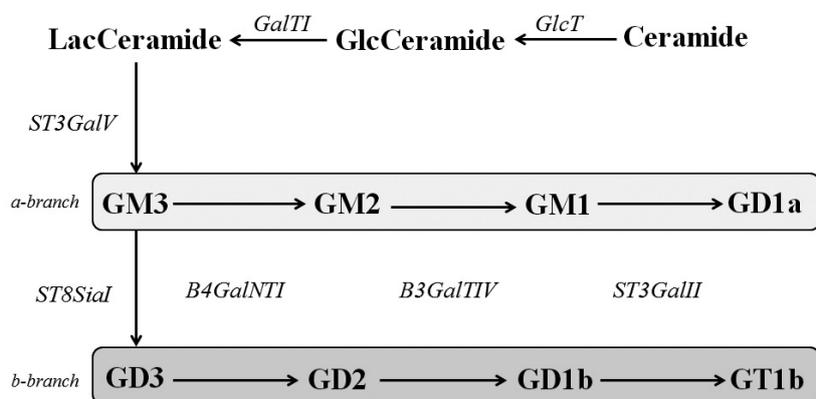

Fig. 1. Scheme of *de novo* biosynthesis of the oligosaccharide moieties of gangliosides

GlcT – UDP-glucose ceramide glucosyltransferase, *GalTI* – UDP-Gal:βGlcNAc β 1,4-galactosyltransferase, *ST3GalV* – ST3 β-galactoside α-2,3-sialyltransferase 5, *ST8SiaI* – ST8 α-N-acetyl-neuraminide α-2,8-sialyltransferase 1, *B4GalNTI* – β-1,4-N-acetyl-galactosaminyl transferase 1, *B3GalTIV* – UDP-Gal:βGlcNAc β 1,3-galactosyltransferase, *ST3GalII* – ST3 β-galactoside α-2,3-sialyltransferase 2.

The aim of the present study was to determine changes in the synthesis and distribution of liver gangliosides following bile duct ligation (BDL), and to assess the effect of the modulation of HMOX activity both on cholestatic liver injury and on ganglioside metabolism.

Material and Methods

Materials

Paraformaldehyde, hemin, biotin, bovine serum albumin (BSA) and diaminobenzidine tetrahydrochloride tablets were supplied by Sigma (St. Louis, MO); avidin was obtained from Fluka (Buchs, Switzerland); the cholera toxin B-subunit (CTB) peroxidase conjugated came from List Biological Laboratories (Campbell, CA). The tin-mesoporfyrin was supplied by Frontier Scientific (Logan, UT). All other chemicals were purchased locally from Penta (Prague, Czech Republic). The TaqMan® Gene Expression Master Mix, High-Capacity RNA-to-cDNA Kit, the TaqMan® Gene Expression Assay kit for rat genes were obtained from Life Technologies (Carlsbad, CA). The QIAshredder kit and RNEasy Plus MiniKit were supplied by Qiagen (Valencia, CA).

Animals and treatments

Female Wistar rats (Anlab, Prague, Czech Republic) were housed under controlled temperature and a natural light-dark cycle. The animals had free access to food and water throughout the experiments, and were fasted overnight prior to the experiment initiation. All aspects of the study met the accepted criteria for the experimental use of laboratory animals, and all protocols were approved by the Animal Research Committee of the First Faculty of Medicine, Charles University in Prague, Czech Republic.

Cholestasis induction

Rats intraperitoneally anaesthetized with ketamine (90 mg/kg) and xylazine (10 mg/kg) underwent ligation or a sham operation. Cholestasis was induced in three groups of rats (N = 8 per group) by microsurgical ligation of segmental bile ducts and resection of the extrahepatic biliary tract ("BDL") (Aller et al., 2004). Biliary trees were exposed through midline abdominal incision. The control group of rats (N = 6) was sham-operated (controls, "C").

HMOX modulation

HMOX was inhibited by a bolus of tin-mesoporphyrin (SnMP) 15 μM/kg administered intraperitoneally on day 1 ("iBDL", BDL with HMOX inhibition; "iC", control with HMOX inhibition) (George et al., 2013; Porteri et al., 2009). Induction of HMOX was performed by a bolus of hemin 30 μM/kg given intraperitoneally on day 0 and day 3 ("aBDL", BDL with HMOX activation; "aC", control with HMOX activation), (Ndisang et al., 2010; Zhong et al., 2010; Muchova et al., 2015).

Tissue preparation

After five days, the inferior vena cava was cannulated through laparotomy, and blood samples were collected (5 ml), transferred to EDTA-containing tubes, mixed, and placed on ice. An aliquot was centrifuged to separate out the plasma. The livers were then harvested and weighed. Pieces of liver tissue were appropriately processed for further biochemical and histochemical analyses (see below). For quantitative histochemical analysis of GM1 ganglioside, the liver specimens were collected using a systematic uniform random sampling method (Hamilton, 1995).

For RNA analysis, 100 mg of tissue was immediately placed in 1.5 ml microfuge tubes containing RNAlater (Qiagen). The tubes were stored at –20 °C until total RNA isolation.

For HMOX activity, HMOX protein, and lipid peroxidation measurements, 100–150 mg of tissue was diluted 1 : 9 (by weight) in 0.1 M potassium phosphate buffer (pH = 7.4), diced, and sonicated with an ultrasonic cell disruptor (Model XL2000, Misonics, Farmingdale, NY). Sonicates were kept on ice and assayed for HMOX activity within 1 hr, or frozen in liquid nitrogen and stored at -80 °C until analysis of the HMOX protein.

Analysis of plasma markers of cholestasis

In order to determine the degree of cholestasis and liver injury, the following plasma levels were assessed: total bile acids (TBA), total bilirubin, alkaline phosphatase (ALP), aspartate aminotransferase (AST), and alanine aminotransferase (ALT). TBA were determined spectrophotometrically using a Bile Acids Kit (Trinity Biotech, Jamestown, NY), while all other markers were quantified in an automatic analyser (Model 717, Hitachi, Tokyo).

HMOX activity measurement

Twenty μl of 10% liver sonicate (2 mg fresh weight [FW]) was incubated for 15 min at 37 °C in carbon monoxide (CO)-free septum-sealed vials containing 20 μl of 150 μM methemalbumin and 20 μl of 4.5 mM NADPH as previously described (Vreman et al., 1999). Blank reaction vials contained 0.1 M phosphate buffer (pH = 7.4) in place of NADPH. Reactions were terminated by adding 5 μl of 30% (w/v) sulphosalicylic acid. The amount of CO generated by the reaction and released into the vial headspace was quantitated by gas chromatography with a reduction gas analyser (Trace Analytical, Menlo Park, CA). HMOX activity was calculated as pmol CO/hr/mg FW.

Isolation and TLC analysis of liver gangliosides

Gangliosides were isolated using the procedure previously described (Majer et al., 2007) and finally purified on a small silica gel column (Yu and Ledeen, 1972). Gangliosides were separated in a solvent system (chloroform/methanol/0.2% aqueous $CaCl_2$, 55/45/10, v/v/v), and detected with resorcinol-HCl reagent. Densitometry

was performed according to Majer et al. (2007). Part of the extract was used for determination of the total sialic acid (total gangliosides) by the photometric method with resorcinol reagent (Svennerholm, 1957).

Light microscopy

Small tissue blocks (about 1 cm³) were fixed in 4% paraformaldehyde followed by the standard procedure for paraffin embedding. Serial sections were cut and stained with haematoxylin and eosin. Each slide was viewed using standard light microscopy.

GM1 histochemistry

GM1 was determined using a modified procedure according to Jirkovska et al. (2007). In brief, 4% formaldehyde was freshly prepared by depolymerization of paraformaldehyde (pH = 7.2). Frozen 6 μm thin sections were first fixed in dry cold acetone (-20 °C) for 15 min, and then in 4% freshly prepared paraformaldehyde for 5 min. Endogenous peroxidase activity was blocked by incubation for 15 min in phosphate-buffered saline (PBS) supplemented with 1% H_2O_2 and 0.1% sodium azide. Endogenous biotin was blocked by means of a DakoCytomation blocking kit (DakoCytomation, Denmark). In order to block nonspecific binding, sections were treated with 3% BSA in PBS for 15 min. GM1 ganglioside in liver sections was detected using CTB biotin labelled (Sigma), diluted 1 : 300 in PBS, plus 3% BSA at 8 °C for 16.5 h, followed with streptavidin-peroxidase polymer at room temperature for 1 h. Peroxidase activity was visualized with diaminobenzidine tetrahydrochloride for 20 min in the dark. Sections were mounted in DAKO S3025 (Dako North America, Inc., Carpinteria, CA). Two negative control tests were performed for each group. First, CTB was omitted in immunohistochemical staining. Second, fixed sections were extracted with chloroform:methanol 2 : 1 at room temperature for 30 min, followed by standard immunohistochemical staining.

Quantitative study of the distribution of GM1 ganglioside in the hepatic lobule

Six liver specimens were used for the experiment. One section of each specimen was used for GM1 ganglioside detection with CTB. In each section, four hepatic lobules with a clearly discernible central vein were selected. In each lobule, one measuring frame in lobular zone II (approximately) was selected for the analysis. The haematoxylin and eosin counterstaining was omitted.

The images of whole sections were photographed at the objective magnification of 40× (NA = 0.12) and stored. The quantity of the reaction product was determined as the mean optical brightness/density of the marked area using the ACC 6.0 image analysis program (SOFO, Brno, Czech Republic). Two different ways were used for quantification. First, the whole section was marked and its mean optical brightness was evaluated.

Second, areas of liver parenchyma in the intermediate (zone II) of the hepatic lobules were marked, and their mean optical brightness was determined separately.

Densitometric analysis of GM1 ganglioside in sinusoidal membrane and adjacent cytoplasm areas

Six liver specimens were used from each animal. One section from each specimen was used for GM1 ganglioside detection as described above. In each section, four hepatic lobules with a clearly discernible central vein were selected. In each lobule, one measuring frame in the central lobular zone III and one measuring frame in the corresponding peripheral lobular zone I were selected for analysis. In each frame, 15 areas of sinusoidal surface and 15 areas of adjacent hepatocyte cytoplasm were selected by the stratified random sampling method (Hamilton, 1995) and marked out. The reaction product was quantified as the mean optical density of the analysed areas (determined by the densitometric program ACC 6.0, SOFO) at objective magnification of 40× (NA = 0.7). The ratios of densities measured in the sinusoidal membrane and subsinusoidal intracellular compartment were measured and compared (sin/int).

Quantitative real-time PCR

The liver samples were stored frozen at –80 °C in RNAlater (Sigma Aldrich, St. Louis, MO), and total RNA was isolated using a Qiagen RNAeasy plus kit and QIAshredder (Qiagen). A High-Capacity cDNA Reverse Transcription Kit (Life Technologies, Carlsbad, CA, USA) was used to generate cDNA. Quantitative real-time PCR was performed using a TaqMan® Gene Expression Assay Kit (Life Technologies for the following genes: *GlcT* (Rn00582480_m1), *GalTI* (Rn00581985_m1), *ST3GalV* (Rn01420866_m1), *ST8SiaI* (Rn00563093_m1), *B4GalNTI* (Rn00575768_m1), *B3GalTIV* (Rn01429268_s1), and β-actin endogenous control kit (Rn00667869_m1), all provided by Life Technologies. The data were normalized to β-actin and expressed as percent of control levels.

Statistical analysis

Normally distributed data are presented as the mean ± SD and analysed by the Student's *t*-test. Medians (25–75%) and the Mann-Whitney U test or Kruskall-Wallis test were used in skewed data. Differences with P < 0.05 were considered significant.

Results

Induction of cholestasis by BDL

As expected, BDL for five days resulted in a significant increase in plasma cholestatic markers, alkaline phosphatase (ALP) activity, as well as BA and bilirubin concentrations (Table 1). Modulation of HMOX activity had no effect on plasma BA levels, while HMOX activation by hemin led to a significant decrease in ALP activ-

Table 1. The effect of BDL on cholestatic markers, and liver and body weight

Group	Body weight [g]	Liver weight [g]	TBA [μmol/l]	Bilirubin [μmol/l]	ALP [μkat/l]	HMOX activity [pmol CO /hr/mg FW]
C (N = 6)	235.5 ± 9.0	10.4 ± 0.7	17.3 ± 9.2	1.4 ± 0.6	2.0 ± 0.3	327.7 ± 48.0
BDL (N = 8)	224.7 ± 16.0	14.5 ± 1.8*	372.0 ± 132.3*	320.5 ± 74.0*	4.4 ± 0.3*	199.4 ± 37.0*
iBDL (N = 8)	209.3 ± 11.0	13.3 ± 1.9	612.6 ± 164.1*†	215.4 ± 47.0*†	3.5 ± 0.9*	59.3 ± 7.0*†
aBDL (N = 8)	218.9 ± 26.0	15.5* ± 1.7	638.4 ± 188.2*†	291.3 ± 38.1*	3.3 ± 0.5*†	640.6 ± 123.0*†

Cholestatic markers, and liver and body weight in Wistar rats 5 days after surgery. C – control, CO – carbon monoxide, FW – fresh weight. * – $P < 0.05$ vs. C; † – $P < 0.05$ vs. BDL

ity (BDL vs. aBDL, $P < 0.05$). Generally, plasma bilirubin levels were substantially affected by its decreased elimination in cholestasis as well as by the changes in its production following induction/inhibition of HMOX. Accordingly, we observed a significant increase in plasma bilirubin levels in all cholestatic groups compared to controls. However, HMOX inhibition in the iBDL group resulted in a significantly lower plasma bilirubin increase compared to the BDL and aBDL groups (Table 1). Compared to controls, BDL, iBDL and aBDL also led to a significant increase in AST activity, a marker of liver injury (data not shown).

The effect of HMOX modulators on enzyme activity was verified by gas chromatography (Table 1). As expected, inhibition of HMOX activity was achieved in the iBDL group, while its increase was detected following HMOX activation in the aBDL group. A significant decrease in HMOX activity was observed in the BDL group compared to controls.

BDL had no effect on the total body weight of the experimental animals. A 15% drop in total body weight was only observed in the iBDL group compared to the controls (Table 1). By contrast, significant increases in liver weight were recorded in all BDL animals compared to the controls.

Modulation of HMOX activity affects ductular proliferation and biliary infarction in obstructive cholestasis

BDL led to typical morphological features of obstructive jaundice in the liver tissue. The histopathological changes included: portal tract expansion, ductular proliferation (mainly in periportal areas), and interlobular bile duct elongation with dilated lumina and irregular epithelium. The surrounding portal tract tissue was oedematous and infiltrated by nonaggressive inflammatory infiltrate, predominantly with neutrophils. Signs of hepatocellular degeneration were observed – feathery degeneration with flocculent cytoplasm and ballooning with swollen hepatocytes. Variable amounts of intracellular bile pigments and focal signs of necrosis with increased hepatocyte regeneration were observed in all BDL rats. Giant cell transformation with coalescence of hepatocytes, multiple nuclei, and free-floating canaliculi were present.
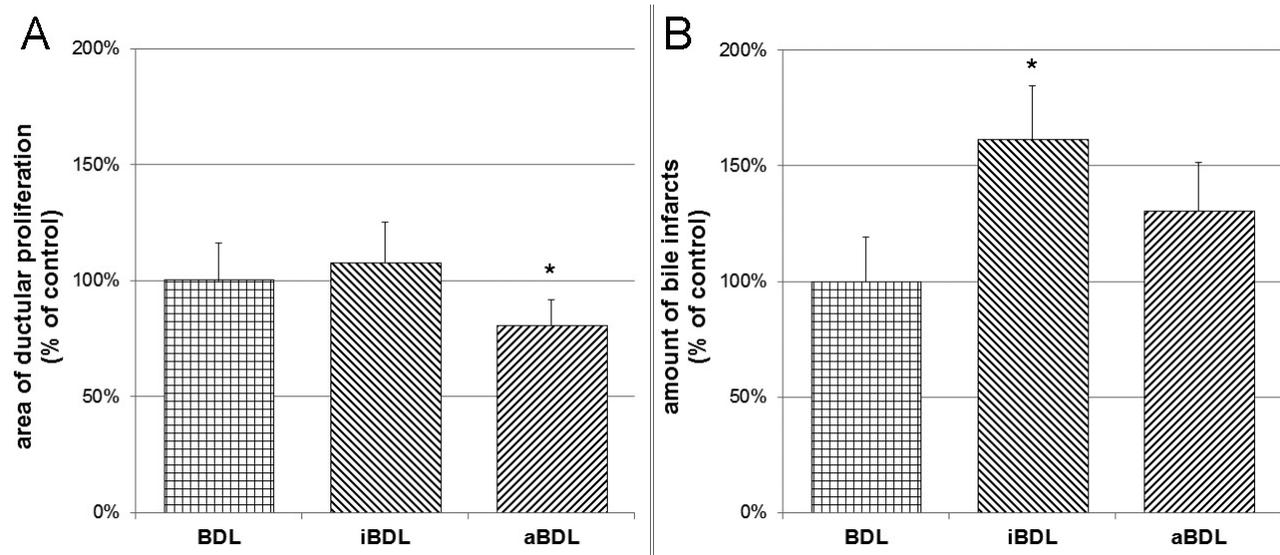

Fig. 2. Area of liver ductular proliferation and number of bile infarcts
A. Area of ductular proliferation in the liver sections of BDL animals. **B**. Number of bile infarcts in liver sections of BDL animals.
Liver sections stained with haematoxylin and eosin were analysed using a systematic uniform random sampling method. Results are expressed as % of controls. * – $P < 0.05$ vs. BDL

HMOX activation resulted in a significant decrease in ductular proliferation (to 83 ± 9 %, P < 0.05), while HMOX inhibition had no effect on ductular proliferation compared to BDL animals (Fig. 2A).

BDL rats developed a typical biliary type of liver cell hepatocyte necrosis with typical bile infarcts. The average number of bile infarcts in BDL rats was 0.43 infarcts per liver section. Inhibition of HMOX significantly increased the amount of bile infarcts compared to BDL controls (0.43 ± 0.11 vs. 0.71 ± 0.09 infarcts per liver section, P < 0.005). In contrast, no effect was observed upon HMOX activation (0.43 ± 0.11 vs. 0.57 ± 0.1 infarcts per section, P > 0.05; Fig. 2B).

BDL and HMOX modulation leads to changes in ganglioside content and spectra

Total lipid sialic acid concentration, a marker of total ganglioside content, was significantly higher in the livers of BDL animals compared to controls (100 ± 20 % vs. 153 ± 15 %, P < 0.001). Inhibition of HMOX activity by SnMP resulted in a further increase in total lipid sialic acid content (298 ± 22 %, P < 0.001). Unfortunately, due to haem interference, we were not able to measure the sialic acid content in the livers of hemin-treated animals (Table 2).

Next, we analysed the hepatic ganglioside spectra of both *a*- and *b*- biosynthetic pathways (Fig. 3A, 3B and Table 3). While the predominant ganglioside was determined to be GM3 in the control livers, GD1a and GD1b were the major gangliosides in the cholestatic livers. Interestingly, HMOX inhibition led to an increase of GM3 ganglioside, while HMOX activation resulted in significant decreases in the liver content of the *b-series* of gangliosides GD1b and GT1b compared to the BDL group (Table 3). Furthermore, obstructive cholestasis was accompanied by a significant increase in the liver ganglioside content, as determined both by thin layer chromatography (Fig. 3A, 3B) and spectrophotometrically as total sialic acid concentration (Table 2). This increase was most pronounced following HMOX inhibition, whereas a tendency to decrease was observed following HMOX activation (Fig. 3A). BDL led to a significant increase in the total amount of di- and trisialogangliosides. In contrast, activation of HMOX led to a significant decrease in these complex gangliosides (Fig. 3B).

Changes in the mRNA expression of the key enzymes of ganglioside metabolism during BDL

To elucidate the biochemical basis of the observed differences in the ganglioside content spectra, we measured the expression of key enzymes involved in ganglioside synthesis – *GlcT*, *GalTI*, *ST3GalV*, *ST8SiaI*, *B4GalNTI* and *B3GalTIV*.

BDL led to a significant increase in *ST3GalV* mRNA expression compared to controls (197 ± 30 %, P < 0.05), (Fig. 4C), and was even more pronounced in iBDL.

Inhibition of HMOX also resulted in a significant increase in *GalTI* (186 ± 22 %, P < 0.001), *ST3GalV,* (371 ± 105 %, P < 0.001), *ST8SiaI* (185 ± 44 %, P < 0.05), and *B3GalTIV* (150 ± 25 %, P < 0.05) mRNA expression compared to the control. The effect of HMOX inhibition in the iBDL group observed as overexpression of *ST3GalV* and *ST8SiaI* was also significant compared to the BDL group (Fig. 4). These results are consistent with the results of TLC ganglioside analysis.

HMOX induction resulted in a significant decrease of *B3GalTIV* expression (68 ± 11 %, P < 0.05; Fig. 4F). Furthermore, a significant drop in *ST3GalV* mRNA expression was observed in the aBDL group when compared to BDL alone.

Table 2. The effect of BDL on total sialic acid concentrations in the liver tissue

Group	C (N = 6)	BDL (N = 8)	iC (N = 6)	iBDL (N = 8)	aC (N = 6)	aBDL (N = 8)
Total sialic acid [nmol/g liver]	17.3 ± 3.5	26.5* ± 3.9	29.3* ± 1.6	51.6*† ± 6.2	N.D.	N.D.

Total sialic acid (total gangliosides) concentrations in the liver tissue of Wistar rats 5 days after surgery was measured by the spectrophotometric method with resorcinol reagent. BDL as well as HMOX inhibition led to a significant increase in total sialic acid content. C – control, N.D. – not determined due to haem interference. * – P < 0.05 vs. C; † – P < 0.05 vs. BDL

Table 3. The effect of BDL on the total amount of gangliosides of the a- and b-branches in the liver tissue

Group	a-Branch [nmol/g liver]			b-Branch [nmol/g liver]		
	GM3	GM1	GD1a	GD3	GD1b	GT1b
C (N = 6)	2.5 ± 0.9	1.01 ± 0.30	2.01 ± 1.40	1.43 ± 0.50	1.04 ± 0.40	0.62 ± 0.20
BDL (N = 8)	2.62 ± 1.10	1.60 ± 0.40*	5.1 ± 1.3*	1.42 ± 0.30	2.86 ± 0.70*	1.49 ± 0.40*
iBDL (N = 8)	3.69 ± 0.70*†	1.91 ± 0.40*	5.89 ± 1.50*	1.85 ± 0.50*	1.81 ± 0.30*	0.91 ± 0.50
aBDL (N = 8)	3.45 ± 1.20	1.83 ± 0.30*	4.31 ± 0.90*	1.49 ± 0.50	1.47 ± 0.40†	0.92 ± 0.20†

Isolated gangliosides were separated in a solvent system and detected with resorcinol-HCl reagent (nmol/g) with subsequent densitometric analysis. BDL led to a significant increase of terminal gangliosides of the *a*- (GD1a and GM1) as well as *b*-branch (GD1b and GT1b).
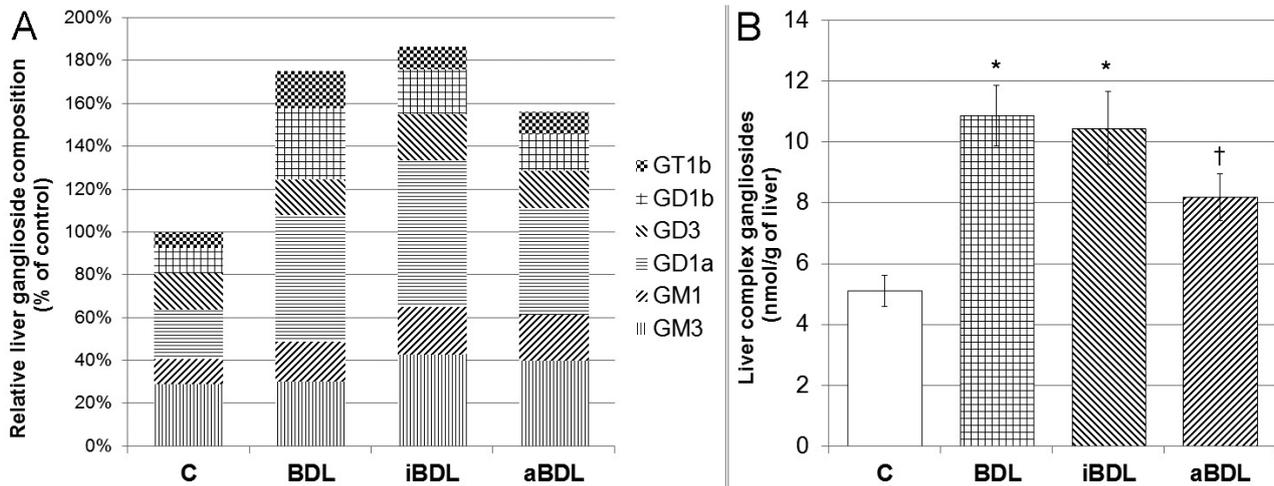C – control, * – P < 0.05 vs. C; † – P < 0.05 vs. BDL

Fig. 3. Effect of BDL on the ganglioside content in the liver
A. Relative amount of gangliosides of the *a*- and *b*-branches in the liver tissue of the control and BDL animals. Isolated gangliosides were separated in a solvent system and detected with resorcinol-HCl reagent, with subsequent densitometric analysis. Results are expressed as % of controls. **B**. Total amount of di- and trisialogangliosides (GD3, GD1, GD1b and GT1b) in the liver tissue of BDL animals.
C – control, [*] – $P < 0.05$ vs. C, [†] – $P < 0.05$ vs. BDL

The shift of GM1 ganglioside to the cytoplasmic membrane during cholestasis is affected by HMOX modulation

Under physiological conditions, the GM1 ganglioside is distributed in both the sinusoidal and canalicular hepatocyte membranes, with strong intracellular localization in all lobular zones in the liver sections of the control animals. The same pattern was observed in the control livers with HMOX modulation (iC and aC), indicating no effect of HMOX modulation on ganglioside distribution within the liver cell under physiological conditions.

However, a marked shift of GM1 positivity from the intracellular compartment to the hepatocyte membrane (predominantly sinusoidal) was observed after BDL ($P < 0.01$, Figs. 5 and 6).

Interestingly, HMOX inhibition in BDL animals resulted in an even more pronounced shift of GM1 to the sinusoidal membrane (iBDL vs. BDL; $P < 0.05$, Fig. 5), whereas no shift of GM1 from the intracellular compartment was observed following HMOX induction in BDL rats, resulting in a similar immunohistological pattern as in the control group (Figs. 5 and 6).

Discussion

In the present study, we showed that cholestasis induced by BDL is accompanied by significant changes both in the distribution and synthesis of the liver gangliosides. Moreover, simultaneous induction of the hepatoprotective and anti-cholestatic HMOX enzyme resulted in attenuation of the cholestatic pattern of liver gangliosides.

Even though gangliosides are considered key structural as well as functional parts of the lipid bilayer, and changes in their chemical composition and cellular concentration might have deleterious consequences (d'Azzo et al., 2006), their pathophysiological significance in the liver tissue needs to be elucidated (Sanchez et al., 2000). Altered ganglioside patterns have been reported in cirrhosis and hepatocellular carcinoma in human livers (Tanno et al., 1988) as well as in biliary cirrhosis in the rat (Senn et al., 1991). A different distribution of ganglioside synthases in hepatocytes, Kupffer cells, and sinusoidal endothelial cells was observed in the rat (Senn et al., 1990). Moreover, our group has demonstrated an altered ganglioside pattern in the livers of rats with EE-induced cholestasis (Jirkovska et al., 2007), and its improvement following HMOX induction by haem (Petr et al., 2014; Muchova et al., 2015).

BDL in rats is used as a model of severe obstructive cholestasis in humans. This disease is characterized by interruption of bile flow, followed by a rapid increase in the plasma levels of BA, conjugated bilirubin, and ALP activity.

As expected, BDL was followed by a severe biochemical as well as histological cholestatic pattern. In accordance with our recent data (Muchova et al., 2011), we observed a decrease in liver HMOX activity as a consequence of the inhibitory effect of high plasma and liver concentrations of BA. In contrast to the study on intrahepatic cholestasis (Muchova et al., 2015), HMOX induction with hemin did not lead to improvement in the plasma cholestatic markers. This might be explained by the different mechanisms of the intrahepatic and obstructive cholestasis. While the primary cause of intrahepatic cholestasis is impaired bile flow due to the changes in hepatocyte transporter expression (Trauner et al., 1997), which might be restored by the effect of haem, the biliary tree obstruction is primarily due to a mechanical obstacle followed by secondary changes in the expression of liver transporters.
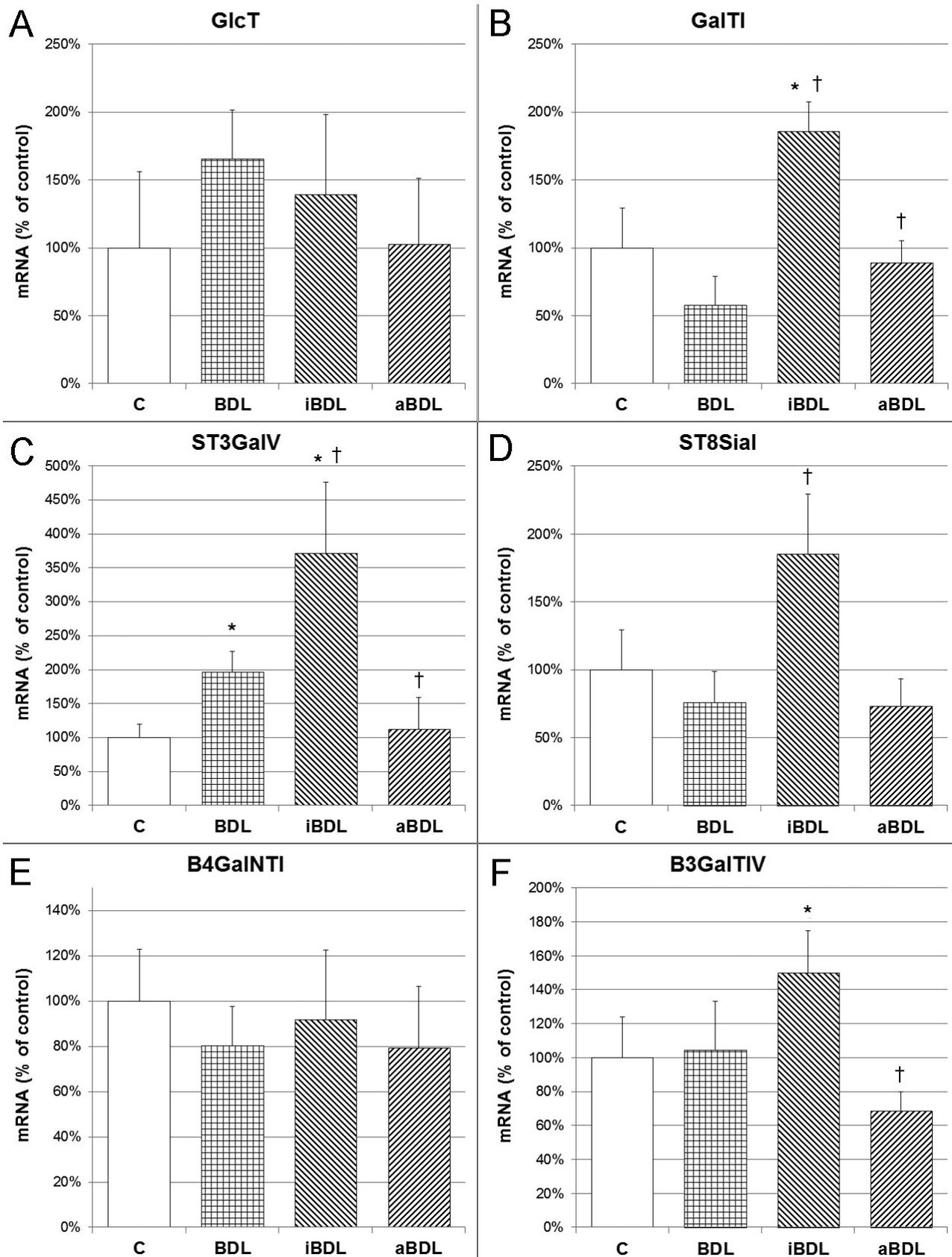
Fig. 4. Effect of BDL on mRNA expression of key enzymes in ganglioside synthesis in the liver
The relative mRNA expression of key glycosyltransferases in ganglioside synthesis was measured in the liver tissue. Results are expressed as % of controls. C – control, * – P < 0.05 vs. C, † – P < 0.05 vs. BDL
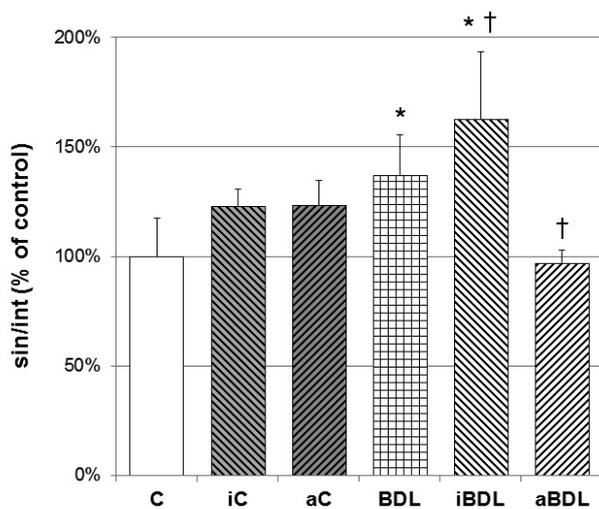
Fig. 5. Distribution of GM1 ganglioside in cholestatic livers Image analysis of the intensity of GM1 ganglioside staining in the subsinusoidal part of the intracellular compartment (int) and sinusoidal membranes (sin) of hepatocytes, expressed as the sin/int ratio. Results are expressed as % of controls. C – control, * – P < 0.05 vs. C, † – P < 0.05 vs. BDL

A significant decrease in ductular proliferation, the hallmark of obstructive cholestasis, was observed in the liver sections of BDL animals with HMOX induction. Cholangiocytes are mitotically dormant in the normal liver, but start to proliferate upon cholangiopathies including BDL (Glaser et al., 2000, Munshi et al., 2011). Two main signalling pathways are involved in cholangiocyte proliferation, the inositol 1,4,5-trisphosphate/Ca^{2+} signalling pathway and cAMP (Alpini et al., 1998). Interestingly, both of these pathways were found to be regulated by gangliosides in different cell culture models (Ravichandra and Joshi, 1999; Kanda et al., 2001).

Moreover, in our study, a significant increase in complex gangliosides (containing at least two sialic acid residues linked to lactosylceramide) was detected in the liver of BDL animals, as well as those with HMOX inhibition compared to controls. In contrast, HMOX activation resulted in a decrease in liver complex gangliosides when compared with BDL without HMOX modulation. Importantly, a completely different role has been attributed to complex versus monosialyl gangliosides in cellular proliferation and differentiation. While monosialyl gangliosides have an anti-proliferative effect, complex gangliosides enhance cell growth and proliferation (Furukawa et al., 2012), indicating that gangliosides might possess an important regulatory role in ductular proliferation in the cholestatic liver. The proliferation of ductules is a logical response of the liver to BA accumulation, which augment the hepatic bile clearance capacity. However, in the case of obstructive cholestasis, these changes are ineffective (the cause of biliary obstruction lies in the common bile duct) and as a consequence, it could have a destructive effect on the liver

parenchyma by replacing the functional hepatocytes by ineffective tissue. In this case, decreasing oxidative stress by hemin administration in cholestasis has a hepatoprotective effect.

The effect of BDL and HMOX modulation on ganglioside synthesis was further supported by determination of mRNA expression of the key enzymes of the ganglioside biosynthesis pathway. BDL animals showed increased *ST3GalV* expression, corresponding to the overall increased ganglioside production from lactosylceramide. HMOX inhibition resulted in a further increase in *ST3GalV,* with simultaneous elevations in *ST8SiaI* and *B3GalTIV,* representing activation of the *b*-branch and terminal gangliosides, respectively. On the other hand, HMOX activation returned the expression of all enzymes to control values. These findings correspond well with the liver ganglioside content as measured by total sialic acid concentrations in the liver, as well as ganglioside spectra in control and cholestatic livers with/without modulation of HMOX.

The accumulation of BA inside hepatocytes is the major cause of cholestatic liver damage (Kullak-Ublick and Meier, 2000), including structural and functional injuries of hepatocyte membranes (Roma et al., 2008), cell death, and activation of inflammatory and fibrogenic signalling pathways (Maher and Friedman, 1993; Muchova et al., 2011). BA may disrupt cell membranes through their detergent action on lipid components and promote generation of ROS, which in turn oxidatively modify lipids, proteins, and nucleic acids; eventually causing hepatocyte necrosis and apoptosis (Perez and Briz, 2009). Recently, it was reported that the canalicular part of the hepatocyte membrane contains detergent-resistant microdomains – lipid rafts – enriched in GSL, including gangliosides, sphingomyelin, and cholesterol, protecting this part of the hepatocyte membrane against the detergent action of BA (Nourissat et al., 2008). There is no doubt that these rafts also exist on the sinusoidal part of the hepatocyte membrane (Zegers and Hoekstra, 1998). Gangliosides as molecules with a high melting point, rigid structure, and highly stable sialic acids are key raft components, responsible for their physical properties.

Recently, Jirkovska et al. (2007) described redistribution of gangliosides within hepatocytes in EE-induced cholestasis. Similarly, in the present study we have shown the shift of the GM1 ganglioside from the intracellular compartment to the sinusoidal membrane of the hepatocyte in cholestatic animals, supporting the concept of a protective effect of gangliosides against the deleterious effect of high plasma levels of BA. Interestingly, this shift was even more pronounced in BDL with HMOX inhibition, while HMOX induction prevented GM1 trafficking to membranes. A similar effect of HMOX induction on ganglioside redistribution was observed by our group (Petr et al., 2014) in the model of EE-induced cholestasis related to reduction of oxidative stress.

We conclude that obstructive cholestasis is accompanied by an increase in the content and synthesis of liver
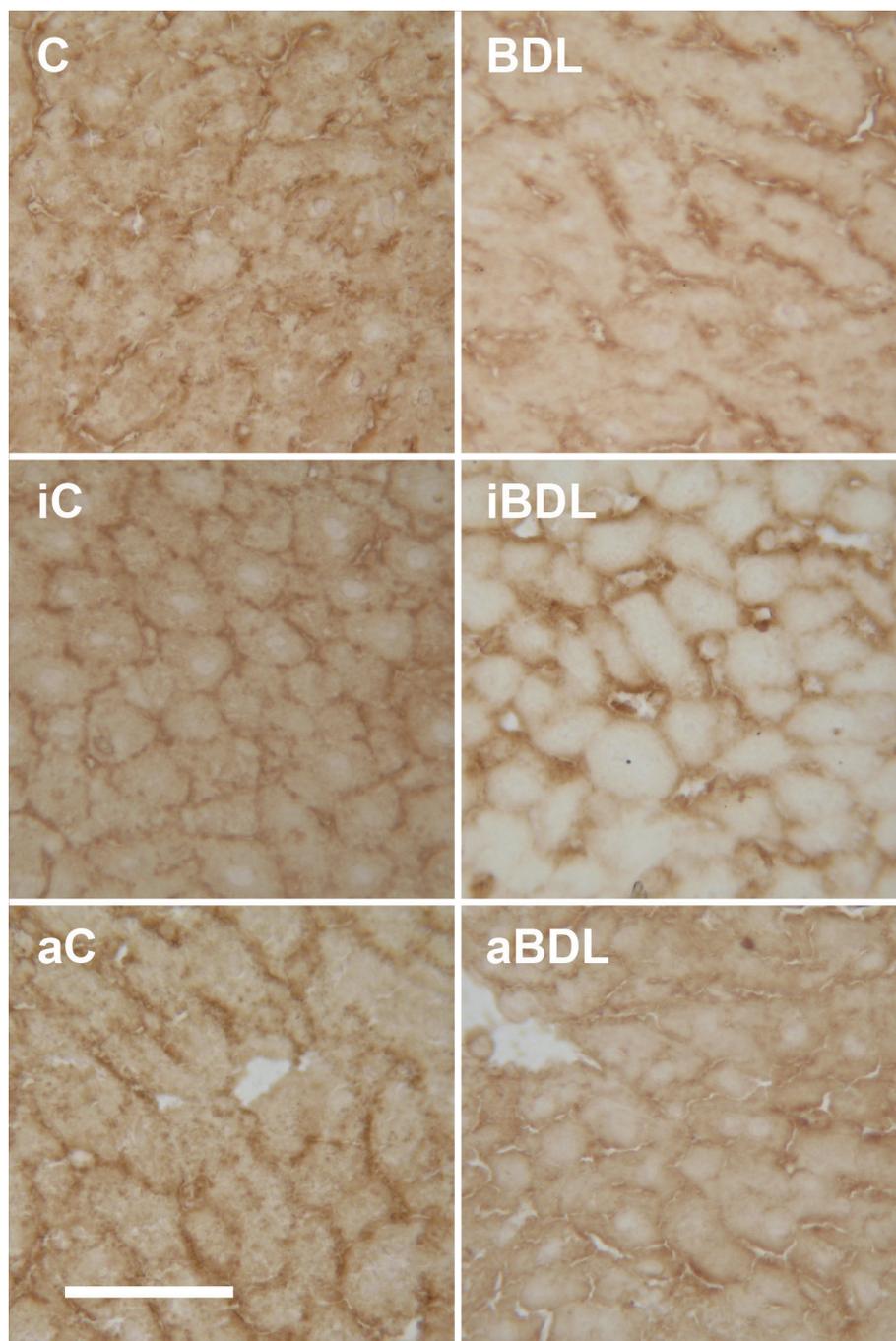
Fig. 6. Localization of GM1 ganglioside in cholestatic livers
In the liver sections, GM1 ganglioside was detected using the cholera toxin B-subunit with streptavidin-peroxidase polymer. Diaminobenzidine tetrahydrochloride (brown colour) was used for visualization. A significant shift of GM1 positivity from the cytoplasm to the sinusoidal membranes was observed after BDL. HMOX inhibition in iBDL animals resulted in an even more pronounced shift of GM1 from the cytoplasm to the sinusoidal membrane, whereas HMOX activation in the aBDL group had the opposite effect. Modulation of HMOX alone in iC and aC had no effect on GM1 localization. C – control. Bar represents 50 μm.

gangliosides followed by their shift into the sinusoidal membranes. This mechanism can protect hepatocytes against the deleterious effect of high systemic concentrations of BA, and also activate proliferation of biliary epithelia. Moreover, the inhibition of antioxidant and hepatoprotective enzyme HMOX in BDL animals further potentiates these changes, while its activation has the opposite effect, indicating the important role of BA-induced oxidative stress in the liver ganglioside metabolism. These results might have potential therapeutic implications, since many drugs and natural products exhibit HMOX-inducing activities (Bach, 2005), and thus might serve as hepatoprotectants.

References

Allen, K., Jaeschke, H., Copple, B. L. (2011) Bile acids induce inflammatory genes in hepatocytes: a novel mechanism of inflammation during obstructive cholestasis. *Am. J. Pathol.* **178**, 175-186.

Aller, M. A., Nava, M. P., Arias, J. L., Duran, M., Prieto, I., Llamas, M. A., Arias, J. (2004) Microsurgical extrahepatic cholestasis in the rat: a long-term study. *J. Invest. Surg.* **17**, 99-104.

Alpini, G., Glaser, S. S., Ueno, Y., Pham, L., Podila, P. V., Caligiuri, A., LeSage, G., LaRusso, N. F. (1998) Heterogeneity of the proliferative capacity of rat cholangiocytes after bile duct ligation. *Am. J. Physiol.* **274**, G767-775.

Bach, F. H. (2005) Heme oxygenase-1: a therapeutic amplification funnel. *FASEB J.* **19**, 1216-1219.

Balistreri, W. F., Leslie, M. H., Cooper, R. A. (1981) Increased cholesterol and decreased fluidity of red cell membranes (spur cell anemia) in progressive intrahepatic cholestasis. *Pediatrics* **67**, 461-466.

Billington, D., Evans, C. E., Godfrey, P. P., Coleman, R. (1980) Effects of bile salts on the plasma membranes of isolated rat hepatocytes. *Biochem. J.* **188**, 321-327.

Boelsterli, U. A., Rakhit, G., Balazs, T. (1983) Modulation by S-adenosyl-L-methionine of hepatic Na^+,K^+-ATPase, membrane fluidity, and bile flow in rats with ethinyl estradiol-induced cholestasis. *Hepatology* **3**, 12-17.

Chester, M. A. (1998) IUPAC-IUB Joint Commission on Biochemical Nomenclature (JCBN). Nomenclature of glycolipids - recommendations 1997. *Eur. J. Biochem.* **257**, 293-298.

d'Azzo, A., Tessitore, A., Sano, R. (2006) Gangliosides as apoptotic signals in ER stress response. *Cell. Death Differ.* **13**, 404-414.

Furukawa, K., Ohkawa, Y., Yamauchi, Y., Hamamura, K., Ohmi, Y. (2012) Fine tuning of cell signals by glycosylation. *J. Biochem.* **151**, 573-578.

George, E. M., Hosick, P. A., Stec, D. E., Granger, J. P. (2013) Heme oxygenase inhibition increases blood pressure in pregnant rats. *Am. J. Hypertens.* **26**, 924-930.

Glaser, S., Benedetti, A., Marucci, L., Alvaro, D., Baiocchi, L., Kanno, N., Caligiuri, A., Phinizy, J. L., Chowdury, U., Papa, E., LeSage, G., Alpini, G. (2000) Gastrin inhibits cholangiocyte growth in bile duct-ligated rats by interaction with cholecystokinin-B/gastrin receptors via D-myo-inositol 1,4,5-triphosphate-, Ca(2+)-, and protein kinase Cα-dependent mechanisms. *Hepatology* **32**, 17-25.

Gujral, J. S., Farhood, A., Bajt, M. L., Jaeschke, H. (2003) Neutrophils aggravate acute liver injury during obstructive cholestasis in bile duct-ligated mice. *Hepatology* **38**, 355-363.

Guyot, C., Stieger, B. (2011) Interaction of bile salts with rat canalicular membrane vesicles: evidence for bile salt resistant microdomains. *J. Hepatol.* **55**, 1368-1376.

Hamilton, P. W. (1995) Designing a morphometric study. In: Hamilton, P. W., Allen, D. C., *Quantitative Clinical Pathology.* Blackwell Science, Cambridge, MA.

Jirkovska, M., Majer, F., Smidova, J., Stritesky, J., Shaik, G. M., Draber, P., Vitek, L., Marecek, Z., Smid, F. (2007) Changes in GM1 ganglioside content and localization in cholestatic rat liver. *Glycoconj. J.* **24**, 231-241.

Kanda, N., Nakai, K., Watanabe, S. (2001) Gangliosides GD1b, GT1b, and GQ1b suppress the growth of human melanoma by inhibiting interleukin-8 production: the inhibition of adenylate cyclase. *J. Invest. Dermatol.* **117**, 284-293.

Kullak-Ublick, G. A., Meier, P. J. (2000) Mechanisms of cholestasis. *Clin. Liver. Dis.* **4**, 357-385.

Maher, J. J., Friedman, S. L. (1993) Parenchymal and non-parenchymal cell interactions in the liver. *Semin. Liver. Dis.* **13**, 13-20.

Majer, F., Trnka, L., Vitek, L., Jirkovska, M., Marecek, Z., Smid, F. (2007) Estrogen-induced cholestasis results in a dramatic increase of b-series gangliosides in the rat liver. *Biomed. Chromatogr.* **21**, 446-450.

Muchova, L., Vanova, K., Zelenka, J., Lenicek, M., Petr, T., Vejrazka, M., Sticova, E., Vreman, H. J., Wong, R. J., Vitek, L. (2011) Bile acids decrease intracellular bilirubin levels in the cholestatic liver: implications for bile acid-mediated oxidative stress. *J. Cell. Mol. Med.* **15**, 1156-1165.

Muchova, L., Vanova, K., Suk, J., Micuda, S., Dolezelova, E., Fuksa, L., Cerny, D., Farghali, H., Zelenkova, M., Lenicek, M., Wong, R. J., Vreman, H. J., Vitek, L. (2015) Protective effect of heme oxygenase induction in ethinylestradiol-induced cholestasis. *J. Cell. Mol. Med.* **19**, 924-933.

Munro, S. (2003) Lipid rafts: elusive or illusive? *Cell* **115,** 377-388.

Munshi, M. K., Priester, S., Gaudio, E., Yang, F., Alpini, G., Mancinelli, R., Wise, C., Meng, F., Franchitto, A., Onori, P., Glaser, S. S. (2011) Regulation of biliary proliferation by neuroendocrine factors: implications for the pathogenesis of cholestatic liver diseases. *Am. J. Pathol.* **178**, 472-484.

Ndisang, J. F., Lane, N., Syed, N., Jadhav, A. (2010) Up-regulating the heme oxygenase system with hemin improves insulin sensitivity and glucose metabolism in adult spontaneously hypertensive rats. *Endocrinology* **151**, 549-560.

Nourissat, P., Travert, M., Chevanne, M., Tekpli, X., Rebillard, A., Le Moigne-Muller, G., Rissel, M., Cillard, J., Dimanche-Boitrel, M. T., Lagadic-Gossmann, D., Sergent, O. (2008) Ethanol induces oxidative stress in primary rat hepatocytes through the early involvement of lipid raft clustering. *Hepatology* **47**, 59-70.

Pascher, I. (1976) Molecular arrangements in sphingolipids. Conformation and hydrogen bonding of ceramide and their implication on membrane stability and permeability. *Biochim. Biophys. Acta* **455**, 433-451.

Pascher, I., Lundmark, M., Nyholm, P. G., Sundell, S. (1992) Crystal structures of membrane lipids. *Biochim. Biophys. Acta* **1113**, 339-373.

Paumgartner, G. (2006) Medical treatment of cholestatic liver diseases: from pathobiology to pharmacological targets. *World J. Gastroenterol.* **12**, 4445-4451.

Perez, M. J., Briz, O. (2009) Bile-acid-induced cell injury and protection. *World J. Gastroenterol.* **15**, 1677-1689.

Petr, T., Smid, V., Kucerova, V., Vanova, K., Lenicek, M., Vitek, L., Smid, F., Muchova, L. (2014) The effect of heme oxygenase on ganglioside redistribution within hepatocytes in experimental estrogen-induced cholestasis. *Physiol. Res.* **63**, 359-367.

Porteri, E., Rodella, L. F., Rezzani, R., Rizzoni, D., Paiardi, S., de Ciuceis, C., Boari, G. E., Foglio, E., Favero, G., Rizzardi, N., Platto, C., Agabiti Rosei, E. (2009) Role of heme oxygenase in modulating endothelial function in mesenteric small resistance arteries of spontaneously hypertensive rats. *Clin. Exp. Hypertens.* **31**, 560-571.

Poss, K. D., Tonegawa, S. (1997) Reduced stress defense in heme oxygenase 1-deficient cells. *Proc. Natl. Acad. Sci. USA* **94**, 10925-10930.

Rajendran, L., Simons, K. (2005) Lipid rafts and membrane dynamics. *J. Cell. Sci.* **118**, 1099-1102.

Ravichandra, B., Joshi, P. G. (1999) Regulation of transmembrane signaling by ganglioside GM1: interaction of anti-GM1 with Neuro2a cells. *J. Neurochem.* **73**, 557-567.

Roma, M. G., Crocenzi, F. A., Sanchez Pozzi, E. A. (2008) Hepatocellular transport in acquired cholestasis: new insights into functional, regulatory and therapeutic aspects. *Clin. Sci. (Lond)* **114**, 567-588.

Sanchez, S. S., Abregu, A. V., Aybar, M. J., Sanchez Riera, A. N. (2000) Changes in liver gangliosides in streptozotocin-induced diabetic rats. *Cell Biol. Int.* **24**, 897-904.

Senn, H. J., Orth, M., Fitzke, E., Scholmerich, J., Koster, W., Wieland, H., Gerok, W. (1990) Altered concentrations, patterns and distribution in lipoproteins of serum gangliosides in liver diseases of different etiologies. *J. Hepatol.* **11**, 290-296.

Senn, H. J., Geiser, T., Fitzke, E., Baumgartner, U., Scholmerich, J., Gerok, W. (1991) Altered biosynthesis of gangliosides in developing biliary cirrhosis in the rat. *J. Hepatol.* **13**, 152-160.

Smith, D. J., Gordon, E. R. (1988) Role of liver plasma membrane fluidity in the pathogenesis of estrogen-induced cholestasis. *J. Lab. Clin. Med.* **112**, 679-685.

Svennerholm, L. (1957) Quantitative estimation of sialic acids. II. A colorimetric resorcinol-hydrochloric acid method. *Biochim. Biophys. Acta* **24**, 604-611.

Tanno, M., Yamada, H., Shimada, H., Ohashi, M. (1988) Ganglioside variations in human liver cirrhosis and hepatocellular carcinoma as shown by two-dimensional thin-layer chromatography. *Clin. Biochem.* **21**, 333-339.

Trauner, M., Arrese, M., Soroka, C. J., Ananthanarayanan, M., Koeppel, T. A., Schlosser, S. F., Suchy, F. J., Keppler, D., Boyer, J. L. (1997) The rat canalicular conjugate export pump (Mrp2) is down-regulated in intrahepatic and obstructive cholestasis. *Gastroenterology* **113**, 255-264.

Trauner, M., Meier, P. J., Boyer, J. L. (1999) Molecular regulation of hepatocellular transport systems in cholestasis. *J. Hepatol.* **31**, 165-178.

Vitek, L., Jirsa, M., Brodanova, M., Kalab, M., Marecek, Z., Danzig, V., Novotny, L., Kotal, P. (2002) Gilbert syndrome and ischemic heart disease: a protective effect of elevated bilirubin levels. *Atherosclerosis* **160**, 449-456.

Vreman, H. J., Wong, R. J., Harmatz, P., Fanaroff, A. A., Berman, B., Stevenson, D. K. (1999) Validation of the Natus CO-Stat End Tidal Breath Analyzer in children and adults. *J. Clin. Monit. Comput.* **15**, 421-427.

Woolbright, B. L., Jaeschke, H. (2012) Novel insight into mechanisms of cholestatic liver injury. *World J. Gastroenterol.* **18**, 4985-4993.

Yu, R. K., Ledeen, R. W. (1972) Gangliosides of human, bovine, and rabbit plasma. *J. Lipid Res.* **13**, 680-686.

Zegers, M. M., Hoekstra, D. (1998) Mechanisms and functional features of polarized membrane traffic in epithelial and hepatic cells. *Biochem. J.* **336 (Pt 2)**, 257-269.

Zhong, W., Xia, Z., Hinrichs, D., Rosenbaum, J. T., Wegmann, K. W., Meyrowitz, J., Zhang, Z. (2010) Hemin exerts multiple protective mechanisms and attenuates dextran sulfate sodium-induced colitis. *J. Pediatr. Gastroenterol. Nutr.* **50**, 132-139.